

The NNLO QCD corrections to Z boson production at large transverse momentum

A. Gehrmann–De Ridder^{a,b,c}, T. Gehrmann^{b,c}, E.W.N. Glover^d, A. Huss^a, T.A. Morgan^d

^a*Institute for Theoretical Physics, ETH, CH-8093 Zürich, Switzerland*

^b*Department of Physics, University of Zürich, CH-8057 Zürich, Switzerland*

^c*Kavli Institute for Theoretical Physics, UC Santa Barbara, Santa Barbara, USA*

^d*Institute for Particle Physics Phenomenology, Department of Physics, University of Durham, Durham, DH1 3LE, UK*

ABSTRACT: The transverse momentum distribution of massive neutral vector bosons can be measured to high accuracy at hadron colliders. The transverse momentum is caused by a partonic recoil, and is determined by QCD dynamics. We compute the single and double-differential transverse momentum distributions for fully inclusive Z/γ^* production including leptonic decay to next-to-next-to-leading order (NNLO) in perturbative QCD. We also compute the same distributions normalised to the cross sections for inclusive Z/γ^* production, i.e. integrated over the transverse momentum of the lepton pair. We compare our predictions for the fiducial cross sections to the 8 TeV data set from the ATLAS and CMS collaborations, which both observed a tension between data and NLO theory predictions, using the experimental cuts and binning. We find that the inclusion of the NNLO QCD effects does not fully resolve the tension with the data for the unnormalised p_T^Z distribution. However, we observe that normalising the NNLO Z -boson transverse momentum distribution by the NNLO Drell–Yan cross section substantially improves the agreement between experimental data and theory, and opens the way for precision QCD studies of this observable.

Contents

1	Introduction	1
2	Setup	3
3	The Z boson transverse momentum distribution	4
4	Double-differential distributions	6
5	Summary and Conclusions	12

1 Introduction

The Drell–Yan production of lepton pairs mediated through a virtual photon or a Z boson is an important process at hadron colliders such as the Large Hadron Collider (LHC). This process has a clean signature with a large event rate, leading to small experimental errors over a wide range of energies. It is a key process in probing Standard Model physics, for example fitting parton distribution functions (PDFs) and measuring the strong coupling constant α_s . Furthermore, it is an important background in searches for signatures of physics beyond the Standard Model, such as supersymmetry and dark matter.

There has been a significant amount of effort to ensure that theoretical predictions match the high precision data available from the LHC. The inclusive cross section for Z/γ^* production is known at NNLO accuracy in QCD [1–4]. Corrections beyond this order have been studied in the soft-virtual approximation [5]. The NNLO QCD corrections have been combined with a resummation of next-to-next-to-leading logarithmic effects (NNLL) [6] which is necessary to predict the transverse momentum distribution of the Z boson at small p_T and matched with parton showers [7]. The NLO electroweak corrections [8, 9] and the mixed QCD–EW corrections [10] have also been computed.

As illustrated in Figure 1, the transverse momentum of the Z boson is generated by the emission of QCD radiation so that the fixed order calculation at $\mathcal{O}(\alpha_s^2)$, which is NNLO for the inclusive cross section, corresponds to only an NLO-accurate prediction of the transverse momentum distribution. The NLO EW corrections to the Z -boson transverse momentum distribution [11] are typically negative and at the level of a few percent at small to moderate p_T^Z , but are enhanced by the well-known electroweak Sudakov logarithms when $p_T^Z \gg M_Z$. At small p_T^Z , the electroweak corrections approach the corrections to the total Z production cross section, such that they largely cancel when normalising the p_T^Z distribution to the total cross section.

Recently the $\mathcal{O}(\alpha_s^3)$ NNLO QCD corrections to Z +jet production were computed [12, 13]. Building upon the calculation presented in Ref. [12], we exploit our highly flexible

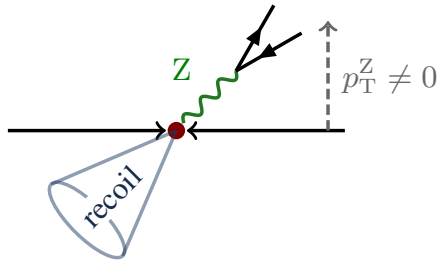


Figure 1. A schematic diagram demonstrating the Z boson recoiling against hard radiation.

and numerically stable code to compute the transverse momentum distribution of the Z boson at finite transverse momentum at NNLO precision. To achieve this we relax the requirement of observing a final state jet and instead impose a low transverse momentum cut on the Z boson. This transverse momentum cut ensures the infrared finiteness of the NNLO calculation, since it enforces the presence of final-state partons to balance the transverse momentum of the Z boson.

The production of Z bosons (or, more generally, of lepton pairs with given invariant mass) at large transverse momentum has been studied extensively at the LHC by the ATLAS [14, 15], CMS [16, 17] and LHCb [18] experiments. In order to reduce the systematic uncertainty on the measurement, the transverse momentum distribution is commonly normalised to the p_T -inclusive Z -boson production cross section. ATLAS and CMS both observed a tension between their measurements and existing NLO QCD predictions, highlighting the potential importance of higher order corrections to this process.

Both experiments present their measurements in the form of fiducial cross sections for a restricted kinematical range of the final state leptons (in invariant mass, transverse momentum and rapidity). In view of a comparison between data and theory, this form of presenting the experimental data is preferable over a cross section that is fully inclusive in the lepton kinematics (requiring a theory-based extrapolation into phase space regions outside the detector coverage). Consequently, the theoretical calculation must take proper account of these restrictions in the final state lepton kinematics.

The unnormalised p_T^Z distribution represents an absolute cross section measurement based on event counting rates. As with any absolute measurement, it has the disadvantage of being sensitive to the proper modelling of acceptance corrections, and of relying on the absolute determination of the integrated luminosity of the data sample under consideration. At the LHC the luminosity uncertainty alone amounts to about 3%. In order to reduce the luminosity uncertainty, the data can be normalised to the Drell–Yan cross section for the corresponding fiducial phase space. This is obtained from the cross section for Z boson production with the same transverse momentum and rapidity cuts on the individual leptons, but integrated over all possible transverse momenta of the Z boson. On the theoretical side, this amounts to normalising the distribution to the NNLO $pp \rightarrow \ell^+ \ell^- + X$ cross section in which the fiducial cuts are applied to the leptons, but which is fully inclusive on the transverse momentum of the lepton-pair.

In this paper, we compute the NNLO QCD corrections to the transverse momentum

distribution for Z production at large transverse momentum, fully inclusive on the accompanying hadronic final state. We present the corrections using the final state cuts used by the ATLAS [15] and CMS [17] collaborations. We study both the absolute (unnormalised) differential cross section and the differential cross section normalised to the relevant Drell–Yan cross section. The NNLO corrections lead to a substantially better theoretical description of the experimental data. We find that the inclusion of the NNLO QCD effects does not fully resolve the tension with the data for the unnormalised p_T^Z distribution. However, we observe that normalising the NNLO Z -boson transverse momentum distribution by the NNLO Drell–Yan cross section leads to an excellent agreement with the experimental distributions.

2 Setup

The NNLO corrections to the production of a Z boson at finite transverse momentum receive contributions from three types of parton-level processes: (a) the two-loop corrections to Z -boson-plus-three-parton processes [19], (b) the one-loop corrections to Z -boson-plus-four-parton processes [20, 21] and (c) the tree-level Z -boson-plus-five-parton processes [21, 22]. The ultraviolet renormalised matrix elements for these processes are integrated over the final state phase space appropriate to Z boson final states, including a cut on the p_T^Z . All three types of contributions are infrared-divergent and only their sum is finite.

In this calculation we employ the antenna subtraction method [23] to isolate the infrared singularities in the different contributions to enable their cancellation prior to the numerical implementation. The construction of the calculation and the subtraction terms is exactly as described in Ref. [12]. All partonic channels relevant to lepton pair production through the exchange of an on-shell or off-shell Z boson or a virtual photon are included. Our calculation is implemented in a newly developed parton-level Monte Carlo generator NNLOJET. This program provides the necessary infrastructure for the antenna subtraction of hadron collider processes at NNLO and performs the integration of all contributing subprocesses at this order. Components of it have also been used in other NNLO QCD calculations [24–27] using the antenna subtraction method. Other processes can be added to NNLOJET provided the matrix elements are available.

To describe the normalised distributions, we also implemented the NNLO QCD corrections to inclusive Z/γ^* production including leptonic decays in NNLOJET, and validated this implementation against the publicly available codes FEWZ [3] and Vrap [4].

For our numerical computations, we use the NNPDF3.0 parton distribution functions (PDFs) [28] with the value of $\alpha_s(M_Z) = 0.118$ at NNLO, and $M_Z = 91.1876$ GeV. Note that we systematically use the same set of PDFs and the same value of $\alpha_s(M_Z)$ for the NLO and NNLO predictions. The factorisation and renormalisation scales are chosen dynamically on an event-by-event basis as,

$$\mu \equiv \mu_R = \mu_F = \sqrt{m_{\ell\ell}^2 + (p_T^Z)^2}, \quad (2.1)$$

where $m_{\ell\ell}$ and p_T^Z are the invariant mass and the transverse momentum of the final state lepton pair respectively. The theoretical uncertainty is estimated by varying the scale

	ATLAS	CMS
leading lepton	$ \eta_{\ell_1} < 2.4$ $p_T^{\ell_1} > 20 \text{ GeV}$	$ \eta_{\ell_1} < 2.1$ $p_T^{\ell_1} > 25 \text{ GeV}$
sub-leading lepton	$ \eta_{\ell_2} < 2.4$ $p_T^{\ell_2} > 20 \text{ GeV}$	$ \eta_{\ell_2} < 2.4$ $p_{T,2}^{\ell_2} > 10 \text{ GeV}$

Table 1. Kinematical cuts used to define the fiducial phase space for the final state leptons in the measurements of ATLAS [15] and CMS [17].

choice by a factor in the range $[1/2, 2]$. The electroweak coupling constant α is derived from the Fermi constant in the G_μ scheme, which absorbs large logarithms of the light fermion masses induced by the running of the coupling constant from the Thomson limit ($Q^2 = 0$) to the electroweak scale into the tree-level coupling. We also impose a cut on the transverse momentum of the Z boson, $p_T^Z > 20 \text{ GeV}$. In the low transverse momentum region, large logarithmic corrections of the form $\log^n(p_T/M_Z)$ appear at each order in the perturbative expansion in α_s , spoiling its convergence. A reliable theoretical prediction in this region can only be obtained by resummation [6] of these logarithms to all orders in perturbation theory. The cut on the transverse momentum also ensures the applicability of our approach, originally developed for Z +jet production at NNLO. In the computation of the inclusive lepton pair production cross section used to normalise the transverse momentum distributions, we choose the same scale (2.1) but varied independently over the same range of scale variation. The inclusive cross section in this case is, however, dominated by the regime where $\mu^2 \approx m_{\ell\ell}^2$.

3 The Z boson transverse momentum distribution

The experimental measurements of Z -boson production at finite transverse momentum are presented in the form of fiducial cross sections over a restricted phase space for the final state leptons, which is fully contained in the detector’s coverage. The NNLO corrections to the transverse momentum distribution can be compared to data by considering the same cuts to the lepton kinematics as presented in the ATLAS [15] and CMS [17] analyses using data from Run 1 of the LHC with $\sqrt{s} = 8 \text{ TeV}$, which are summarised in Table 1. In this section we will focus on the ATLAS measurement in the fiducial region defined by a broad dilepton invariant mass window around the Z resonance, $66 \text{ GeV} < m_{\ell\ell} < 116 \text{ GeV}$, and compare both the absolute and normalised p_T^Z distribution to the experimental data.

Figure 2 shows a comparison of data from the ATLAS analysis within this fiducial region. At low transverse momentum, the NNLO correction increases the cross section by about 6% (compared to NLO) and significantly reduces the scale uncertainty. However, there is still significant tension between the ATLAS data and the NNLO prediction.

The data presented in Figure 2 does not include the error on the integrated luminosity, which amounts to an overall normalisation uncertainty of 2.8% on all data points. To cancel the luminosity uncertainty from the measured data, it is more appropriate to normalise

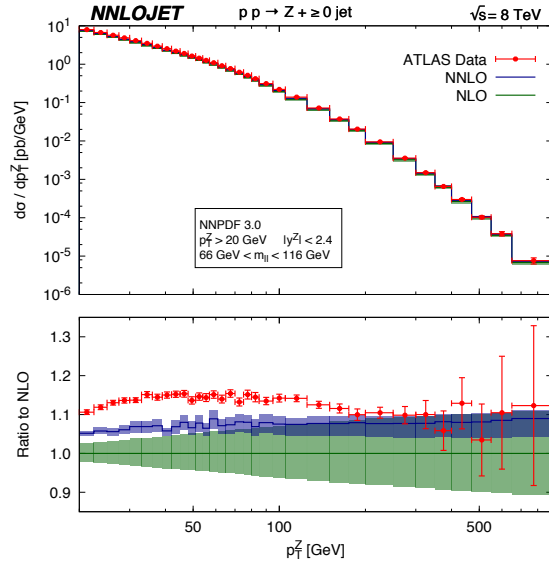


Figure 2. The unnormalised Z -boson transverse momentum distribution for the cuts given in Table 1 and $66 \text{ GeV} < m_{\ell\ell} < 116 \text{ GeV}$. ATLAS data is taken from Ref. [15]. The luminosity error is not shown. The green bands denote the NLO prediction with scale uncertainty and the blue bands show the NNLO prediction with scale uncertainty.

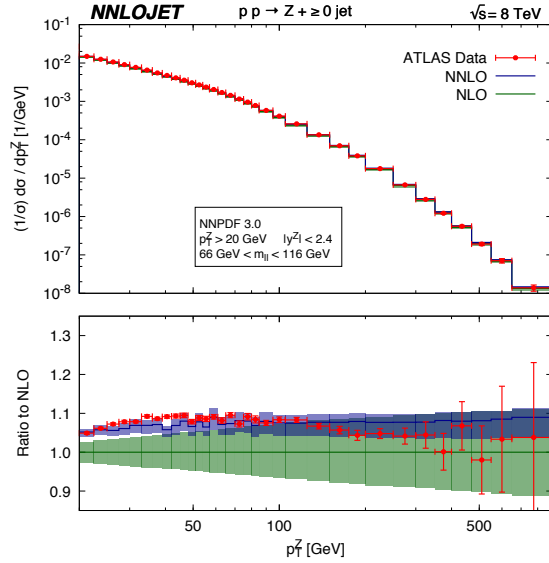


Figure 3. The normalised Z -boson transverse momentum distribution for the cuts given in Table 1 and $66 \text{ GeV} < m_{\ell\ell} < 116 \text{ GeV}$. ATLAS data is taken from Ref. [15]. The green bands denote the NLO prediction with scale uncertainty and the blue bands show the NNLO prediction with scale uncertainty.

the data by the measured values for the inclusive lepton pair cross section in this fiducial bin. The cross section for this mass window was measured to be [15],

$$\sigma_{\text{exp}}(66 \text{ GeV} < m_{\ell\ell} < 116 \text{ GeV}) = 537.10 \pm 0.45\% \text{ (sys.)} \pm 2.80\% \text{ (lumi.) pb.}$$

For the NNLO prediction of the cross section in this fiducial region, we obtain,

$$\sigma_{\text{NNLO}}(66 \text{ GeV} < m_{\ell\ell} < 116 \text{ GeV}) = 507.9_{-0.7}^{+2.4} \text{ pb.}$$

We see that there is some tension between the measured cross section compared to the theoretical result. The normalised distribution is presented in Figure 3, where excellent agreement is observed between the normalised NNLO prediction and the experimental data across a wide range of transverse momentum. The scale bands on the normalised theory predictions are obtained by independently varying the scale in the numerator and denominator, where we use the NNLO prediction for the inclusive Drell–Yan cross section in the normalisation throughout.

The electroweak corrections to this distribution are known to be small at moderate transverse momenta but become more sizeable in the high- p_T^Z tail where they can reach $\sim -15\%$ for $p_T^Z \gtrsim 600 \text{ GeV}$ [11]. It can be therefore expected that the inclusion of electroweak corrections will further improve the prediction of the shape in the tail. However, this region of the distribution is still dominated by the statistical uncertainties of the experimental data and a fully consistent inclusion of electroweak corrections is beyond the scope of this work.

4 Double-differential distributions

We now compare our theoretical predictions for dilepton production at large transverse momentum for different ranges of (a) the dilepton mass and (b) the dilepton rapidity. These double-differential distributions have also been studied by ATLAS [15] and CMS [17] with Run 1 data using the lepton rapidity and transverse momentum cuts summarised in Table 1.

We first consider the ATLAS measurement, which covers a broader kinematical range. In Figure 4 we present the unnormalised double-differential distribution with respect to the transverse momentum of the Z boson and the invariant mass of the lepton pair, $m_{\ell\ell}$, normalised to the NLO prediction and compare it to the ATLAS data from Ref. [15]. We observe that there is good agreement between the NNLO prediction and the data in the low $m_{\ell\ell}$ mass windows. For values of $m_{\ell\ell}$ close to the Z boson mass, where the statistical accuracy of the data is highest, the NNLO prediction is below the data by about 5-8%.

To obtain normalised distributions, these data sets are divided by the inclusive dilepton cross sections for each fiducial bin, defined by the lepton cuts given in Table 1 and the appropriate dilepton invariant mass cut. We computed these fiducial cross sections to NNLO accuracy ($\mathcal{O}(\alpha_s^2)$) and compare them to the measured values quoted by ATLAS [15] in Figure 5. We clearly observe that the central value of the NNLO prediction falls below the experimental data in all mass bins. The large scale dependence in the three lowest mass bins can be explained from the interplay between the cuts on the lepton pair invariant mass and on the single lepton transverse momentum. The latter cuts forbid events at low transverse momentum of the lepton pair down to $m_{\ell\ell} = 40 \text{ GeV}$, such that the two lowest bins receive no leading order contribution, and the third bin only a very small one. All three bins are populated only from NLO onwards, with events containing a low-mass lepton pair recoiling

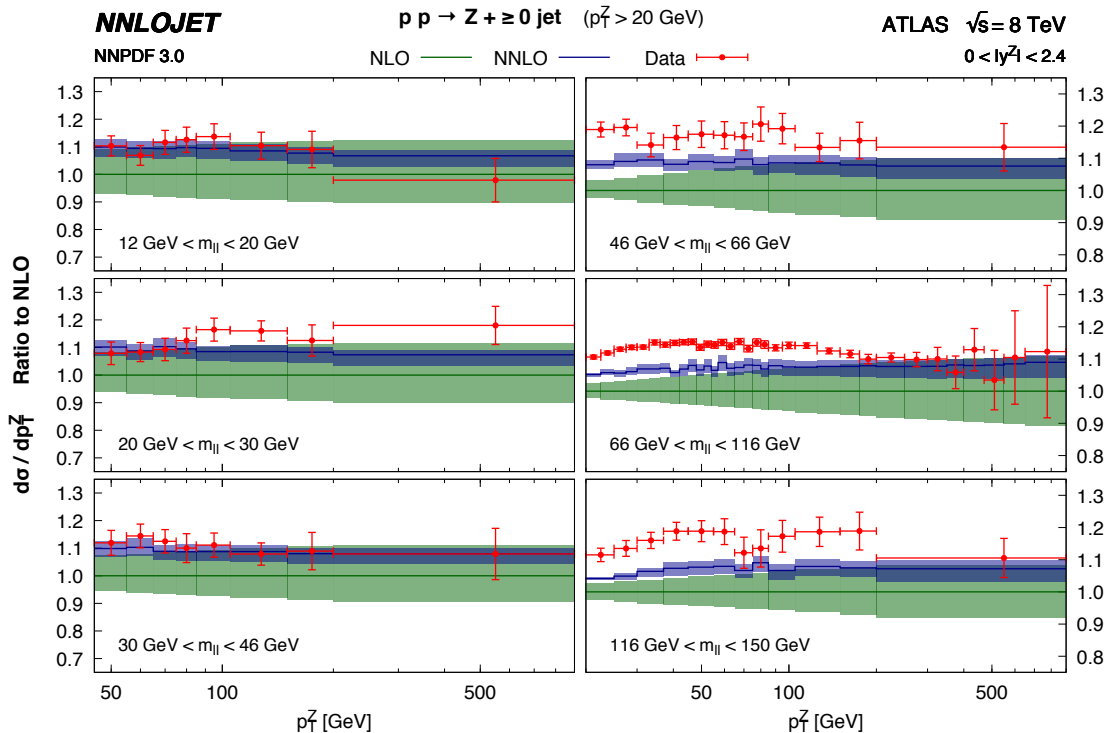


Figure 4. The unnormalised double-differential transverse momentum distribution for the Z boson in windows of invariant mass of the leptons, $m_{\ell\ell}$, with a rapidity cut on the Z boson of $|y^Z| < 2.4$. The ATLAS data is taken from Ref. [15]. The luminosity error is not shown. The green bands denote the NLO prediction with scale uncertainty and the blue bands show the NNLO prediction with scale uncertainty.

against a parton at high transverse momentum. So our NNLO prediction for the inclusive cross section in these mass bins is effectively only NLO accurate, with consequently larger scale dependence. In the three bins with larger $m_{\ell\ell}$, the scale uncertainty on the NNLO prediction is below 0.7%, which results in tension between data and theory at the level of two standard deviations.

Combining together the unnormalised differential distribution with the inclusive cross sections, we obtain the normalised distributions shown in Figure 6. Because of the large scale uncertainty in the inclusive cross section, the theoretical errors dominate the low $m_{\ell\ell}$ bins. At large $m_{\ell\ell}$, the tension between the data and NNLO theory is largely relieved. At the highest values of p_T^Z , the tendency of the data to fall below the theory prediction may be an indication of the onset of electroweak corrections [11], which are negative in this region. Any remaining tension for medium values of p_T^Z could potentially be accounted for revisiting the parton distribution functions (especially the gluon distribution) in the kinematical region relevant to this measurement.

The same tension between NNLO theory and ATLAS data for the unnormalised distribution is visible in Figure 7, which shows the unnormalised double-differential distribution with respect to the transverse momentum of the Z boson for $66 \text{ GeV} < m_{\ell\ell} < 116 \text{ GeV}$

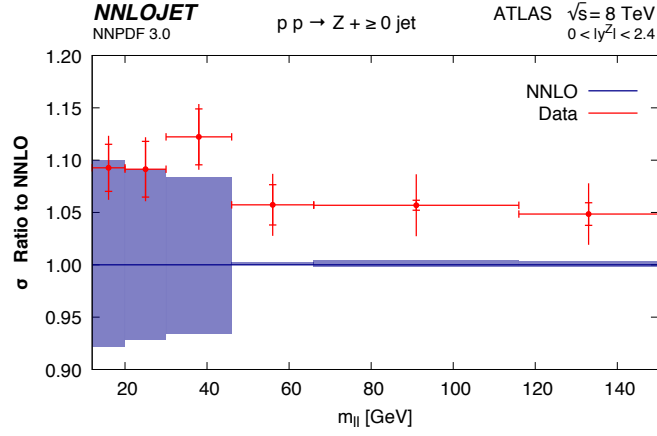


Figure 5. The inclusive dilepton cross section for the same $m_{\ell\ell}$ bins as in Figure 4 and with a rapidity cut on the Z boson of $|y^Z| < 2.4$. The experimental data is taken from the ATLAS analysis in Ref. [15]. The ticks on the vertical error bands denote the systematic uncertainty from the measurement, the vertical bars without the ticks are the luminosity uncertainty only. The blue bands show the NNLO prediction with scale uncertainty.

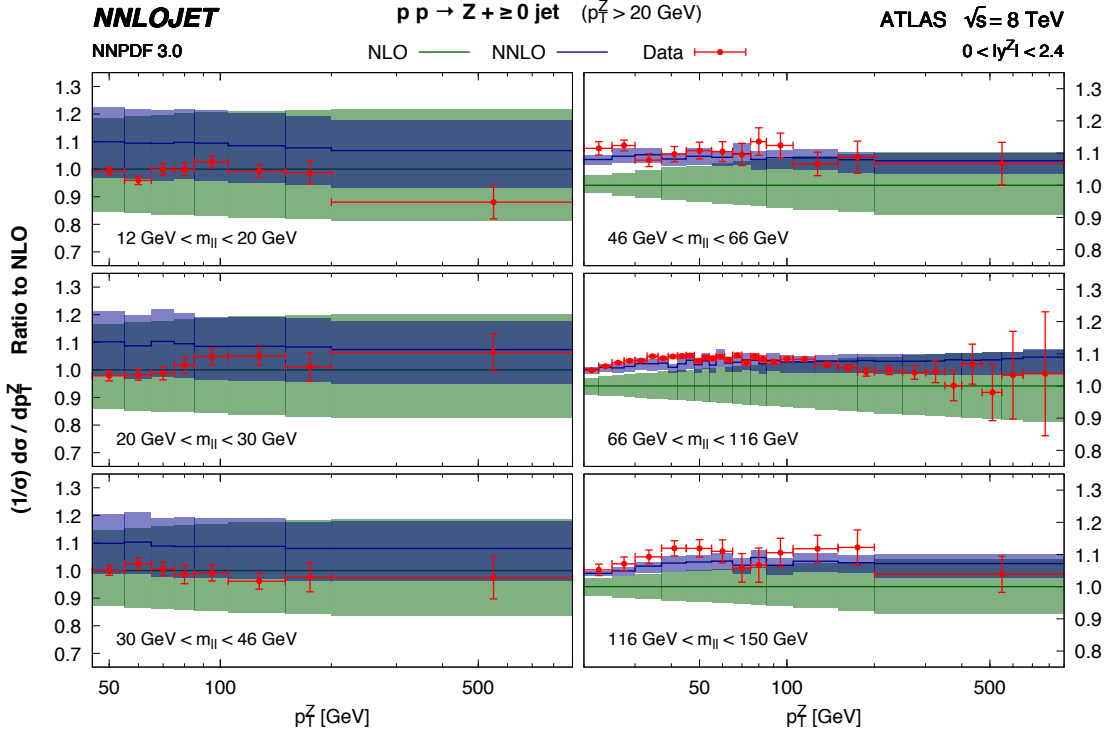


Figure 6. The normalised double-differential transverse momentum distribution for the Z boson in windows of invariant mass of the leptons, $m_{\ell\ell}$, with a rapidity cut on the Z boson of $|y^Z| < 2.4$. The ATLAS data is taken from Ref. [15]. The green bands denote the NLO prediction with scale uncertainty and the blue bands show the NNLO prediction with scale uncertainty.

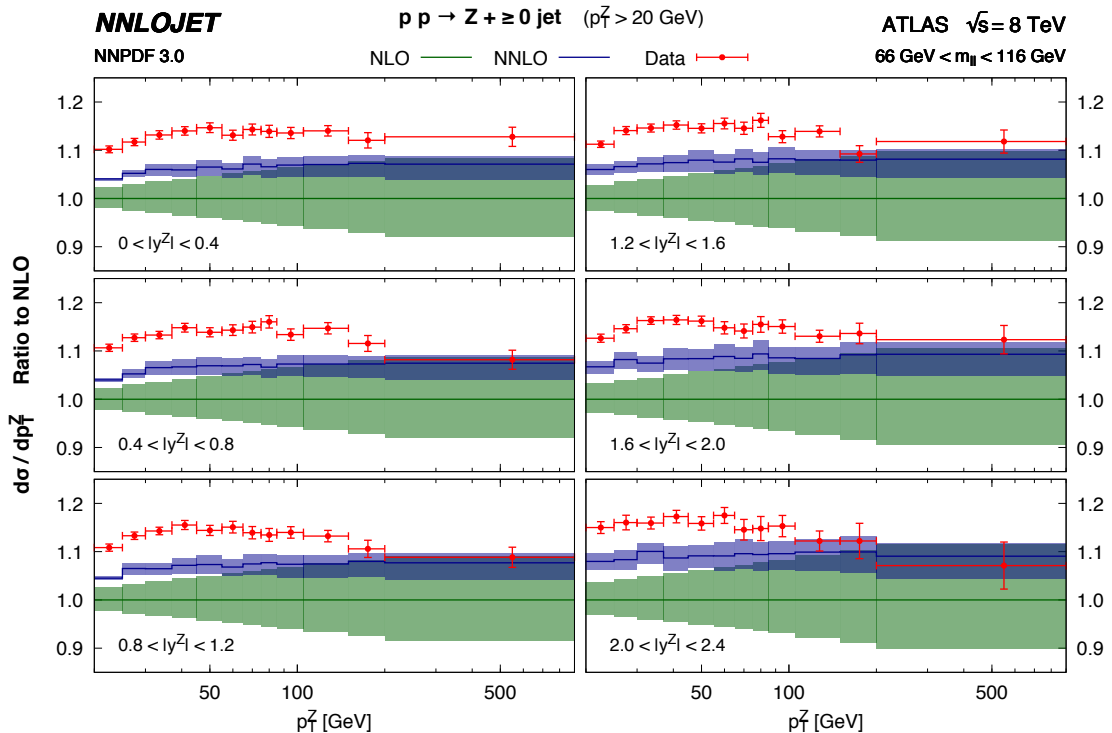


Figure 7. The unnormalised double-differential transverse momentum distribution for the Z boson in windows of rapidity of the Z boson, y^Z , with an invariant mass cut on the final state leptons of $66 \text{ GeV} < m_{\ell\ell} < 116 \text{ GeV}$. The ATLAS data is taken from Ref. [15]. The luminosity error is not shown. The green bands denote the NLO prediction with scale uncertainty and the blue bands show the NNLO prediction.

in different ranges of the rapidity of the Z boson, normalised to the NLO prediction. The NNLO corrections are uniform in rapidity and transverse momentum at the level of about 5–8%, and they decrease the residual theoretical uncertainty to 2–4%. The data, which correspond to the invariant mass bin containing the Z resonance, are consistently above the NNLO prediction.

In order to eliminate the overall luminosity uncertainty, one again normalises the data to the inclusive fiducial dilepton cross section in the respective bins in y^Z . Figure 8 shows the ratio of ATLAS data and the NNLO cross section compared to the NLO prediction¹. As for the rapidity-integrated cross section in this mass bin, Figure 5, we observe the NNLO prediction to be accurate to 0.9%, and to underestimate the ATLAS data by about two standard deviations. The normalised double-differential distribution is shown in Figure 9. There is excellent agreement between the normalised NNLO prediction and the ATLAS data for all rapidity bins, again offering the possibility of further constraining the PDFs in this kinematic region.

¹Note that the ATLAS data is extracted from Ref. [15] by summing the bins of the p_T^Z distributions in the various y^Z bins. We have checked that this procedure applied to the different $m_{\ell\ell}$ bins shown in Figure 5 correctly reproduces the data.

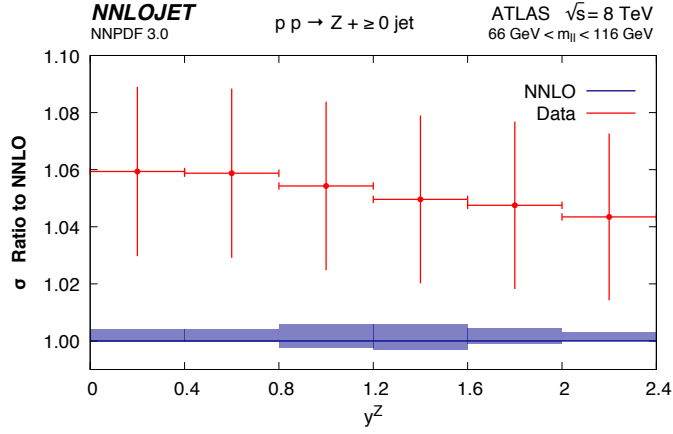


Figure 8. The inclusive dilepton cross section for the same $|y^Z|$ bins as in Figure 7 and an invariant mass cut on final state leptons of $66 \text{ GeV} < m_{\ell\ell} < 116 \text{ GeV}$. The ATLAS data is extracted from Ref. [15] by summing up the transverse momentum distributions in the respective bins. The vertical error bars are given by the luminosity uncertainty. The blue bands show the NNLO prediction with scale uncertainty.

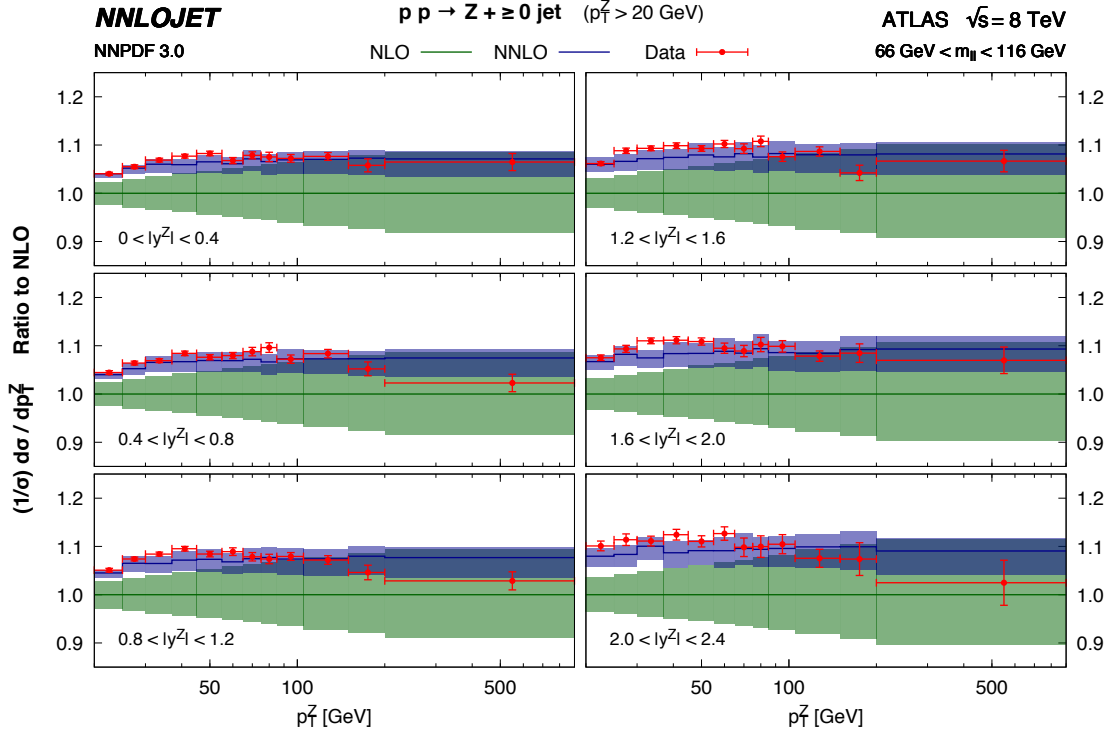


Figure 9. The normalised double-differential transverse momentum distribution for the Z boson in windows of rapidity of the Z boson, y^Z , with an invariant mass cut on final state leptons of $66 \text{ GeV} < m_{\ell\ell} < 116 \text{ GeV}$. The ATLAS data is taken from Ref. [15]. The green bands denote the NLO prediction with scale uncertainty and the blue bands show the NNLO prediction.

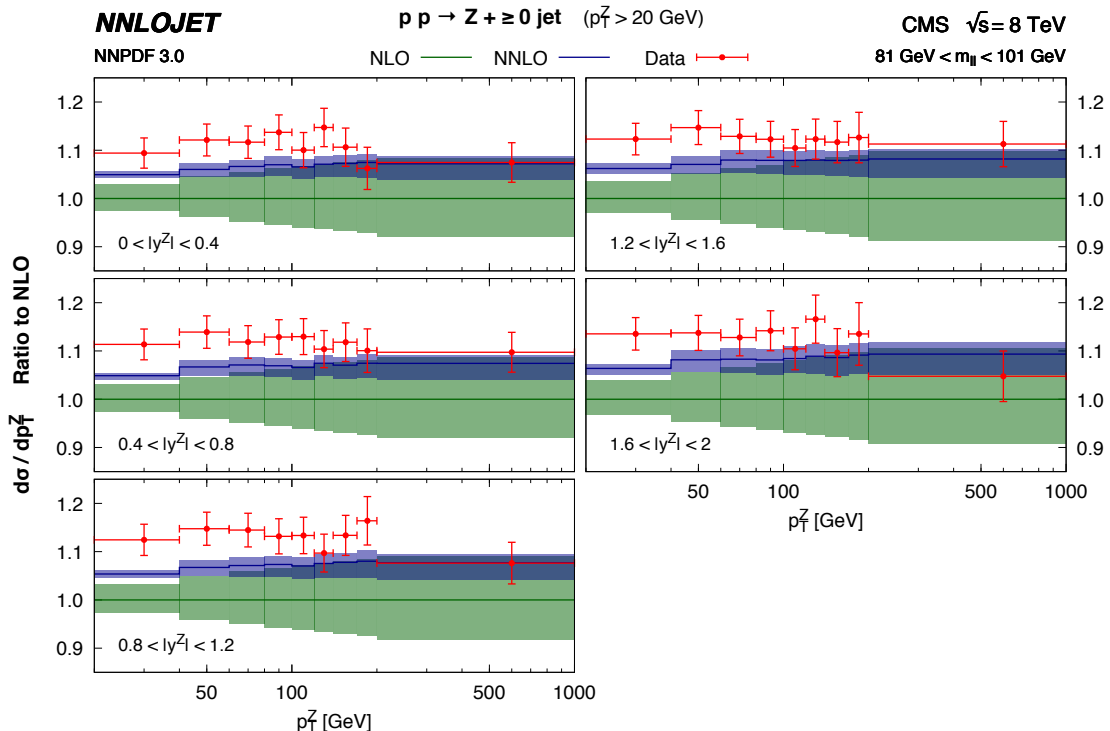


Figure 10. The unnormalised double-differential transverse momentum distribution for the Z boson in windows of rapidity of the Z boson, y^Z , with an invariant mass cut on final state leptons of $81 \text{ GeV} < m_{\ell\ell} < 101 \text{ GeV}$. The CMS data is taken from Ref. [17]. The luminosity error is not shown. The green bands denote the NLO prediction with scale uncertainty and the blue bands show the NNLO prediction.

The CMS measurement of the Z -boson transverse momentum distribution at 8 TeV [17] concentrates on the dilepton invariant mass range $81 \text{ GeV} < m_{\ell\ell} < 101 \text{ GeV}$ around the Z resonance. The fiducial region of this measurement, defined in Table 1, applies asymmetric cuts on the leading and sub-leading lepton, disregarding the lepton charge. To ensure the correct implementation of these cuts in NNLOJET, and to maintain local cancellations between matrix elements and subtraction terms in the antenna subtraction method, the lepton identification as leading and sub-leading had to be passed alongside the lepton charge through all subtraction terms and into the event analysis routines. The double-differential measurement is performed in p_T^Z and y^Z . Comparing the absolute double-differential distributions of Figure 10 to our NNLO predictions, we observe the same features as for the ATLAS measurement, with positive NNLO corrections at the level of 5–8% and an NNLO scale uncertainty of 2–4%. Compared to NLO, inclusion of NNLO corrections brings the theoretical prediction closer to the experimental data, which are however still about 5–8% larger than expected from theory.

In the CMS study [17], the normalised cross section is obtained by dividing the distributions by the fiducial cross section integrated over all bins in y^Z (in contrast to ATLAS, which normalised to the fiducial cross sections only integrated over the respective bin in

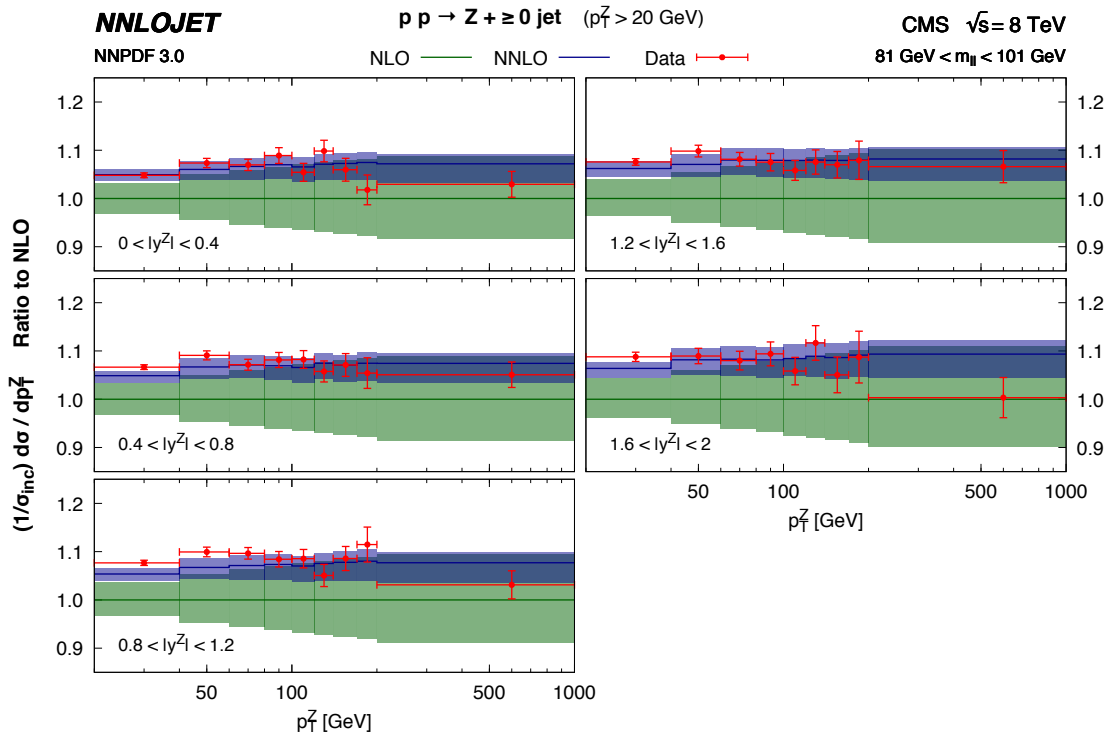


Figure 11. The normalised double-differential transverse momentum distribution for the Z boson in windows of rapidity of the Z boson, y^Z , with an invariant mass cut on final state leptons of $81 \text{ GeV} < m_{\ell\ell} < 101 \text{ GeV}$. The CMS data is taken from Ref. [17]. The green bands denote the NLO prediction with scale uncertainty and the blue bands show the NNLO prediction.

y^Z). At NNLO, we obtain for the fiducial cross section with CMS cuts:

$$\sigma_{\text{NNLO}}(81 \text{ GeV} < m_{\ell\ell} < 101 \text{ GeV}) = 450.6_{-1.6}^{+2.7} \text{ pb.}$$

The normalised distributions of CMS are compared to theory in Figure 11, where excellent agreement is observed upon inclusion of the NNLO corrections.

Compared to NNLO theory, both ATLAS and CMS fiducial cross section measurements of the Z -boson transverse momentum display a similar pattern of disagreement for the absolute distributions while having excellent agreement for the normalised distributions. The inclusion of the newly derived NNLO corrections to the transverse momentum distribution are crucial for a meaningful comparison between data and theory: (a) they reduce the theory uncertainty to a level that firmly establishes the discrepancy on the absolute cross sections, and (b) they modify the central value and the shape of the theory prediction to better agree with the data on the normalised distributions.

5 Summary and Conclusions

We have derived the NNLO QCD corrections to the production of Z/γ^* bosons decaying to lepton pairs at large transverse momentum, inclusive over the hadronic final state.

This observable has typically been very easy to measure but difficult to predict theoretically because of the necessity to be fully inclusive with respect to all QCD radiation. Our calculation is performed using the parton-level Monte Carlo generator NNLOJET which implements the antenna subtraction method for NNLO calculations of hadron collider observables. It extends our earlier calculation of Z/γ^* +jet production at this order [12] and now also includes inclusive Z/γ^* production. We have performed a thorough comparison of theory predictions to the 8 TeV Run 1 data of the LHC for cross sections defined over a fiducial region of lepton kinematics from the ATLAS [15] and CMS [17] collaborations. We observe that the NNLO corrections to the unnormalised distributions are moderate and positive, resulting in theory predictions that are closer to the experimental observations than at NLO. However, this improvement is much more dramatic when one considers distributions normalised to the relevant dilepton cross section. This is true for both single and double-differential distributions. While the normalised distributions for low $m_{\ell\ell}$ slices in comparison to ATLAS are dominated by the theoretical scale uncertainty on the inclusive dilepton cross section, for larger $m_{\ell\ell}$ and all $|y^Z|$ bins the agreement between NNLO theory and LHC data is excellent. With the reduction of the theoretical scale uncertainty at NNLO, a careful reinvestigation of the parametric ingredients to the NNLO theory predictions (parton distributions, strong coupling constant, electroweak parameters) appears now to be mandatory. Our calculation enables exactly these precision studies, and will allow a consistent inclusion of the precision data on the Z transverse momentum distribution into NNLO determinations of parton distributions, leading to precision constraints at this order on the gluon distribution over a large momentum range.

Acknowledgments

We would like to thank Daniel Froidevaux and Elzbieta Richter-Was for stimulating discussions concerning the ATLAS data, Dieter Zeppenfeld for enlightening comments that helped to shape the phenomenological study in this paper and Alexander Mück for helpful comments concerning the impact of EW corrections to these observables. We also thank Xuan Chen, Juan Cruz-Martinez, James Currie and Jan Niehues for useful discussions and their many contributions to the NNLOJET code. This research was supported in part by the National Science Foundation under Grant NSF PHY11-25915, in part by the Swiss National Science Foundation (SNF) under contracts 200020-162487 and CRSII2-160814, in part by the UK Science and Technology Facilities Council, in part by the Research Executive Agency (REA) of the European Union under the Grant Agreement PITN-GA-2012-316704 (“HiggsTools”) and the ERC Advanced Grant MC@NNLO (340983).

References

- [1] R. Hamberg, W. L. van Neerven and T. Matsuura, Nucl. Phys. B **359** (1991) 343 [Nucl. Phys. B **644** (2002) 403]. W. L. van Neerven and E. B. Zijlstra, Nucl. Phys. B **382** (1992) 11 [Nucl. Phys. B **680** (2004) 513]. C. Anastasiou, L. J. Dixon, K. Melnikov and F. Petriello, Phys. Rev. Lett. **91** (2003) 182002 [hep-ph/0306192]; K. Melnikov and F. Petriello, Phys. Rev.

- Lett. **96** (2006) 231803 [hep-ph/0603182]; Phys. Rev. D **74** (2006) 114017 [hep-ph/0609070]; S. Catani, G. Ferrera and M. Grazzini, JHEP **1005** (2010) 006 [arXiv:1002.3115 [hep-ph]];
- [2] S. Catani, L. Cieri, G. Ferrera, D. de Florian and M. Grazzini, Phys. Rev. Lett. **103** (2009) 082001 [arXiv:0903.2120 [hep-ph]].
- [3] R. Gavin, Y. Li, F. Petriello and S. Quackenbush, Comput. Phys. Commun. **182** (2011) 2388 [arXiv:1011.3540 [hep-ph]].
- [4] C. Anastasiou, L. J. Dixon, K. Melnikov and F. Petriello, Phys. Rev. D **69** (2004) 094008 doi:10.1103/PhysRevD.69.094008 [hep-ph/0312266].
- [5] S. Moch and A. Vogt, Phys. Lett. B **631** (2005) 48 [hep-ph/0508265]. E. Laenen and L. Magnea, Phys. Lett. B **632** (2006) 270 [hep-ph/0508284]. A. Idilbi, X. d. Ji and F. Yuan, Nucl. Phys. B **753** (2006) 42 [hep-ph/0605068]. V. Ravindran and J. Smith, Phys. Rev. D **76** (2007) 114004 [arXiv:0708.1689 [hep-ph]]. T. Ahmed, M. Mahakhud, N. Rana and V. Ravindran, Phys. Rev. Lett. **113** (2014) 11, 112002 [arXiv:1404.0366 [hep-ph]]. D. Bonocore, E. Laenen, L. Magnea, L. Vernazza and C. D. White, Phys. Lett. B **742** (2015) 375 [arXiv:1410.6406 [hep-ph]].
- [6] J. C. Collins, D. E. Soper and G. F. Sterman, Nucl. Phys. B **250** (1985) 199; G. Bozzi, S. Catani, G. Ferrera, D. de Florian and M. Grazzini, Nucl. Phys. B **815** (2009) 174 [arXiv:0812.2862 [hep-ph]]; Phys. Lett. B **696** (2011) 207 [arXiv:1007.2351 [hep-ph]]; T. Becher and M. Neubert, Eur. Phys. J. C **71** (2011) 1665 [arXiv:1007.4005 [hep-ph]].
- [7] A. Karlberg, E. Re and G. Zanderighi, JHEP **1409** (2014) 134 [arXiv:1407.2940 [hep-ph]]; S. Höche, Y. Li and S. Prestel, Phys. Rev. D **91** (2015) 074015 [arXiv:1405.3607 [hep-ph]].
- [8] U. Baur, O. Brein, W. Hollik, C. Schappacher and D. Wackerroth, Phys. Rev. D **65** (2002) 033007 [hep-ph/0108274]. V. A. Zykunov, Phys. Rev. D **75** (2007) 073019 [hep-ph/0509315]. C. M. Carloni Calame, G. Montagna, O. Nicrosini and A. Vicini, JHEP **0710** (2007) 109 [arXiv:0710.1722 [hep-ph]].
- [9] L. Barze, G. Montagna, P. Nason, O. Nicrosini, F. Piccinini and A. Vicini, Eur. Phys. J. C **73** (2013) 6, 2474 [arXiv:1302.4606 [hep-ph]].
- [10] S. Dittmaier, A. Huss and C. Schwinn, Nucl. Phys. B **885** (2014) 318 [arXiv:1403.3216 [hep-ph]]; S. Dittmaier, A. Huss and C. Schwinn, arXiv:1511.08016 [hep-ph].
- [11] J. H. Kühn, A. Kulesza, S. Pozzorini and M. Schulze, Nucl. Phys. B **727** (2005) 368 [hep-ph/0507178]; A. Denner, S. Dittmaier, T. Kasprzik and A. Mück, JHEP **1106** (2011) 069 [arXiv:1103.0914 [hep-ph]]; W. Hollik, B. A. Kniehl, E. S. Scherbakova and O. L. Veretin, Nucl. Phys. B **900** (2015) 576 doi:10.1016/j.nuclphysb.2015.09.018 [arXiv:1504.07574 [hep-ph]].
- [12] A. Gehrmann-De Ridder, T. Gehrmann, E. W. N. Glover, A. Huss and T. A. Morgan, arXiv:1507.02850 [hep-ph]; arXiv:1601.04569 [hep-ph].
- [13] R. Boughezal, J. M. Campbell, R. K. Ellis, C. Focke, W. T. Giele, X. Liu and F. Petriello, Phys. Rev. Lett. **116** (2016) 152001 [arXiv:1512.01291 [hep-ph]]; R. Boughezal, X. Liu and F. Petriello, arXiv:1602.05612 [hep-ph]; arXiv:1602.08140 [hep-ph].
- [14] G. Aad *et al.* [ATLAS Collaboration], JHEP **1409** (2014) 145 [arXiv:1406.3660 [hep-ex]].
- [15] G. Aad *et al.* [ATLAS Collaboration], arXiv:1512.02192 [hep-ex].
- [16] S. Chatrchyan *et al.* [CMS Collaboration], Phys. Rev. D **85** (2012) 032002 [arXiv:1110.4973 [hep-ex]].

- [17] V. Khachatryan *et al.* [CMS Collaboration], Phys. Lett. B **749** (2015) 187 [arXiv:1504.03511 [hep-ex]].
- [18] R. Aaij *et al.* [LHCb Collaboration], JHEP **1508** (2015) 039 [arXiv:1505.07024 [hep-ex]]; JHEP **1601** (2016) 155 [arXiv:1511.08039 [hep-ex]].
- [19] L. W. Garland, T. Gehrmann, E. W. N. Glover, A. Koukoutsakis and E. Remiddi, Nucl. Phys. B **627** (2002) 107 [hep-ph/0112081]; Nucl. Phys. B **642** (2002) 227 [hep-ph/0206067]; T. Gehrmann and L. Tancredi, JHEP **1202** (2012) 004 [arXiv:1112.1531 [hep-ph]].
- [20] E. W. N. Glover and D. J. Miller, Phys. Lett. B **396** (1997) 257 [hep-ph/9609474]; Z. Bern, L. J. Dixon, D. A. Kosower and S. Weinzierl, Nucl. Phys. B **489** (1997) 3 [hep-ph/9610370]; J. M. Campbell, E. W. N. Glover and D. J. Miller, Phys. Lett. B **409** (1997) 503 [hep-ph/9706297]; Z. Bern, L. J. Dixon and D. A. Kosower, Nucl. Phys. B **513** (1998) 3 [hep-ph/9708239].
- [21] J. M. Campbell and R. K. Ellis, Phys. Rev. D **65** (2002) 113007 [hep-ph/0202176]; J. M. Campbell, R. K. Ellis and D. L. Rainwater, Phys. Rev. D **68** (2003) 094021 [hep-ph/0308195].
- [22] K. Hagiwara and D. Zeppenfeld, Nucl. Phys. B **313** (1989) 560; F. A. Berends, W. T. Giele and H. Kuijf, Nucl. Phys. B **321** (1989) 39; N. K. Falck, D. Graudenz and G. Kramer, Nucl. Phys. B **328** (1989) 317.
- [23] A. Gehrmann-De Ridder, T. Gehrmann and E. W. N. Glover, JHEP **0509** (2005) 056 [hep-ph/0505111]; Phys. Lett. B **612** (2005) 49 [hep-ph/0502110]; Phys. Lett. B **612** (2005) 36 [hep-ph/0501291]. A. Daleo, T. Gehrmann and D. Maitre, JHEP **0704** (2007) 016 [hep-ph/0612257]; A. Daleo, A. Gehrmann-De Ridder, T. Gehrmann and G. Luisoni, JHEP **1001** (2010) 118 [arXiv:0912.0374]; T. Gehrmann and P.F. Monni, JHEP **1112** (2011) 049 [arXiv:1107.4037]; R. Boughezal, A. Gehrmann-De Ridder and M. Ritzmann, JHEP **1102** (2011) 098 [arXiv:1011.6631]; A. Gehrmann-De Ridder, T. Gehrmann and M. Ritzmann, JHEP **1210** (2012) 047 [arXiv:1207.5779]; J. Currie, E.W.N. Glover and S. Wells, JHEP **1304** (2013) 066 [arXiv:1301.4693 [hep-ph]].
- [24] A. Gehrmann-De Ridder, T. Gehrmann, E.W.N. Glover and G. Heinrich, JHEP **0711** (2007) 058 [arXiv:0710.0346 [hep-ph]]; Comput. Phys. Commun. **185** (2014) 3331 [arXiv:1402.4140 [hep-ph]].
- [25] A. Gehrmann-De Ridder, T. Gehrmann, E.W.N. Glover and J. Pires, Phys. Rev. Lett. **110** (2013) 162003 [arXiv:1301.7310 [hep-ph]]; J. Currie, A. Gehrmann-De Ridder, E.W.N. Glover and J. Pires, JHEP **1401** (2014) 110 [arXiv:1310.3993 [hep-ph]].
- [26] G. Abelof, A. Gehrmann-De Ridder and I. Majer, JHEP **1512** (2015) 074 [arXiv:1506.04037 [hep-ph]].
- [27] X. Chen, T. Gehrmann, E.W.N. Glover and M. Jaquier, Phys. Lett. B **740** (2015) 147 [arXiv:1408.5325 [hep-ph]].
- [28] R. D. Ball *et al.* [NNPDF Collaboration], JHEP **1504** (2015) 040 [arXiv:1410.8849 [hep-ph]].